Optical simulation model of the diffuse reflectance near-infrared spectroscopy for predicting fresh maize quality

Yongli Zhang[1,2*], Meipan Wang[2,3], Guanghui Yang[2,3], Jian Li[1,2], Guangfei Zhu[1,2], Jianfang Shi[1,2], Tailin Han[3], Xuan Liu[3*]

(1. *Academy of Agricultural Planning and Engineering, Ministry of Agriculture and Rural Affairs, Beijing 100125, China*; 2. *Key Laboratory of Agro-Products Primary Processing, Ministry of Agriculture and Rural Affairs, Beijing 100125, China*; 3. *College of Electronic Information Engineering, Changchun Science and Technology University, Changchun 130000, China*)

Abstract: The optical properties of fresh maize tissues determine how light interacts with fresh maize cobs, which in turn affects the measured spectral signals and model accuracy. In this paper, a simulation model was developed to invert the optical properties of fresh maize cobs and evaluate the effects of different optical layouts on the accuracy of modeling predictions. First, the uniformity of detector irradiation at various distances (10 mm, 20 mm, 30 mm, 40 mm, 50 mm) and angles (30°, 45°, 60°) with different optical properties was analyzed using optical simulation methods. Then, the spectra of fresh maize cobs were collected at different light source angles and detection distances, and the spectral area polarization was calculated. Finally, the optical properties of the cob were estimated by establishing a link between irradiation uniformity and spectral area polarization, which resolved the distribution of light flux in edible maize cobs under different optical structures. The results show that the model of light transport mimicking the organizational structure of maize cob has been successfully simulated. The estimated optical properties of the cob are: absorption A=37%, transmission T=20%, and diffuse reflectance D=40%. This verifies that the accuracy and precision of the prediction model for the water content of fresh maize are best achieved under an optical structure with a detection distance of 40 mm and a light source angle of 45°. The establishment of the simulation model provides theoretical support for near-infrared detection of the intrinsic quality of fresh maize.

Keywords: fresh maize cob, optical properties, Monte Carlo simulation, diffuse reflectance spectrum, optical structure

DOI: 10.25165/j.ijabe.20251806.9484

Citation: Zhang Y L, Wang M P, Yang G H, Li J, Zhu G F, Shi J F, et al. Optical simulation model of the diffuse reflectance near-infrared spectroscopy for predicting fresh maize quality. Int J Agric & Biol Eng, 2025; 18(6): 250–259.

1 Introduction

Fresh maize combines the characteristics of grain, fruit, and vegetable, offering high nutritional value and good taste. China ranks first in the world for both the production and consumption of fresh maize, with the planting area exceeding 1.34 million hectares in recent years[1,2]. However, the grade classification of fresh maize remains confusing.

Near-infrared spectroscopy is widely used for detecting the internal quality of agricultural products because it allows for the acquisition of information and the evaluation and analysis of the intrinsic quality of specimens without destroying the samples. Near infrared spectroscopy technology is the use of fruit and vegetable tissues to measure the Near Infrared (NIR) reflection, scattering, transmission, and absorption characteristics, which can reflect the internal tissue composition information of fruits and vegetables. For example, it can measure the soluble solid content of korla fragrant pears[3], the moisture content of walnut kernels[4], and the soluble sugar content in super sweet maize[5]. Additionally, near-infrared spectroscopy has been widely used for non-destructive quality evaluation of agricultural products, such as detecting the ripeness of pineapple pulp[6] and identifying mold in walnuts[7]. Recently, NIR spectroscopy techniques have relied on chemometrics for modeling and analyzing signals and agricultural quality indicators[8]. However, NIR measurements describe the combined effect of absorption and scattering, which cannot separate the absorption and scattering effects, weakening the ability to reflect the structural properties of tissues and easily leading to the loss of key information, which creates difficulties and challenges in the accuracy, stability, and versatility of prediction models[9-11]. Optical characterization helps to understand the mechanism of interaction between light and fruits and vegetables, providing information related to physical structure (particle size, shape, distribution density) and chemical composition (moisture, soluble solids content)[12-15], and thus providing a theoretical basis for quality testing of agricultural products.

So far, many scholars have explored the optical properties of fruits and vegetables. Pan et al.[16] studied a method for detecting the quality of fruits and vegetables based on optical characteristic parameters, finding that this method is very effective for quality detection applications. Fruits and vegetables are complex turbid organisms that cause multilayer scattering of light in transmission, and Monte Carlo model theory is often used to study the transmission properties of light energy in biological tissues. Monte

Received date: 2024-11-08 **Accepted date:** 2025-07-24

Biographies: Meipan Wang, Undergraduate Student, research interest: signal detection, Email: 2979527260@qq.com; **Guanghui Yang**, Undergraduate Student, research interest: signal detection, Email: y0119gh@163.com; **Jian Li**, PhD, Senior Engineer, research interest: processing of agricultural products, Email: lj15408@163.com; **Guangfei Zhu**, PhD, Senior Engineer, research interest: processing of agricultural products, Email: sjf-yb@163.com; **Jianfang Shi**, Senior Engineer, research interest: processing of agricultural products, Email: zhuguangfei@aape.org.cn; **Tailin Han**, PhD, Professor, research interest: Signal Processing, Email: hantl@cust.edu.cn.

***Corresponding author: Yongli Zhang**, PhD, Engineer, research interest: agricultural product inspection and grading, Academy of Agricultural Planning and Engineering, Ministry of Agriculture and Rural Affairs, Beijing 100125, China. Tel: +86-010-59197323, Email: Lalizhang@163.com; **Xuan Liu**, PhD, Associate Professor, research interest: signal processing, Changchun Science and Technology University, Changchun 130000, China. Email: woliuxuan1@163.com.

Carlo simulation can effectively deal with the complex propagation behavior of light in inhomogeneous media, which is often difficult to accurately describe with traditional analytical methods[17]. Instead of solving the radiative transfer equation, the Monte Carlo (MC) method estimates the optical properties of tissues by simulating the process of light propagation through a medium, and is a computational technique used to understand the interaction of photons with tissues[18]. Tan et al.[19] used Monte Carlo simulation of a three-layer kernel model to evaluate the effects of probe geometry and fiber parameters on near-infrared spectral measurements. Zhang et al.[20] used the Monte Carlo method to simulate photon trajectories within apples and then applied this method to real apple sample data for learning and prediction, enabling them to analyze the characteristics of the apple kernel layer through the simulated luminosity map. These studies have demonstrated that Monte Carlo methods can effectively invert the optical properties of fruits and vegetables. However, there are few studies exploring the inversion of optical properties specifically for fresh maize cobs in the existing literature on maize.

According to Tan et al.[21], existing optical inversion models are based on the assumption that the turbid medium is homogeneous and semi-infinite. In reality, fruit and vegetable tissues exhibit various geometrical shapes, while the Monte Carlo method is a purely numerical calculation that does not account for these geometric influences. As a result, achieving accurate optical resolution is challenging. This study proposed a new approach to address the problem of low optical resolution accuracy. LightTools and SolidWorks software were used to construct the geometric shape and optical structure of maize cob, while Monte Carlo simulation was employed to achieve the optical inversion of the maize cob.

LightTools is an optical simulation software based on Monte Carlo simulation, which can effectively simulate the photon transport process in non-homogeneous media (e.g. biological tissues). Models of fruit and vegetable tissues can be defined according to practical applications. Fruit and vegetable tissues usually consist of different layers of tissues, such as skin in the outermost layer, pulp in the middle layer, and core in the innermost layer. Each layer of tissue has different optical properties (absorption, scattering, transmission)[22]. Vaudelle et al.[23] used Monte Carlo simulations to model the propagation properties of light inside and at the boundaries of two layers of apple tissue, modeling the apples as two centrally homogeneous spheres, with radii differing only by an amount equal to the thickness of the skin, while the inner layer contains the pulp. LightTools can define the optical properties of different layer organizations and simulate the propagation of light through different layers. The software provides a variety of scattering models to describe the propagation of photons in non-homogeneous media, the common ones being the Lambertian scattering model and the Gaussian scattering model. The Lambertian model is applied to ideal diffusely reflecting surfaces, assumes that the intensity of light scattering is uniformly distributed in all directions, and only light absorption is considered, while scattering effects are neglected[24]; Gaussian scattering models, on the other hand, are suitable for describing the non-uniform scattering of light in inhomogeneous media, and are particularly suitable for the simulation of light propagation in complex structures such as biological tissues[25]. Through Monte Carlo simulation, LightTools can trace the propagation paths of photons through different layers and tissues, simulate their absorption, scattering and reflection processes, and statistically analyze the transmission, reflection, and scattering characteristics of light in each media layer. It is possible to view the distribution of light energy in different tissue structures and assess the absorption and scattering of light in each layer[26-28]. Therefore, LightTools is able to fulfill the simulation needs of the cob spectral detection system. In order to improve the efficiency of detecting vascular browning (VAB) detection in apples, Sun et al.[29] used LightTools software to build two different optical geometries of NIR measurement devices and perform ray tracing; this simulation study shows the suitable optical layout for internal defect detection. Han et al.[30] used LightTools to establish a model for optical detection of water-core apples and compared the optical structures of two- and four-light sources. It was found that a detection system with a four-light source layout could mitigate the effects of apple size and water core distribution on the prediction of SSC and WSI.

Combined with an actuality spectral acquisition device, this study simplifies the fresh maize cob tissue model. A detection system was established in which photons are emitted from a halogen lamp, propagated through the cob tissue, and then captured by an optical fiber. The uniformity of detector irradiation was observed under different optical structures. The aim is to gain a better understanding of internal quality testing methods for fruits and vegetables based on spectral analysis techniques. This approach ultimately enhances the resolution of spectral features and verifies model accuracy. The purpose of this paper is to analyze the mechanism of interaction between near-infrared light and fresh maize cob materials, and to provide theoretical basis for the detection mechanism and the design of detection system for nondestructive testing of the intrinsic quality of fresh maize cobs.

2 Materials and methods

2.1 Simulation modeling process

In the simulation modeling, maize cob, halogen lamp, and fiber optic probe were modeled in three dimensions using SolidWorks software. Then, the model was transferred to LightTools 8.6 software for optical simulation, as shown in Figure 1a. The fiber optic probe in the simulation model is simplified as a straight model. A receiver is placed on the receiving surface of the fiber optic probe to collect light data, to evaluate the luminous flux received by the probe under different optical structures, and to calculate the irradiation uniformity of its receiving surface. In the process of three-dimensional modeling of fresh maize cob, a model of the mid-section of maize cob with surface texture information was established. In the modeling of the detection system, the model was appropriately simplified according to the characteristics of the actual system. Based on the structure of halogen lamps, a model of a lamp cup type halogen lamp was constructed, and the light source was simplified to a surface light source, focused at the origin. In the specific structure modeling, the parameters are set for each component as shown in Figure 2. The diameter of the receiving surface (d) is 0.5 mm, the detection angle (θ) is set to 12.5°, and the specific structure is shown in Figure 2a. The halogen lamp simplifies the light source as a surface light source and sets the focal point to be located at the coordinate origin, and the light-emitting parameters are set according to the data provided by the manufacturer, in which the luminous flux (I) is 200 lm and the light-emitting angle (ϕ) is 180°, as shown in Figure 2b. According to the actual physical dimensions and structural characteristics of the cob of fresh maize, a three-dimensional model of the middle part of the cob was established, with the radius of the cob (R) of 50 mm, the length of the kernel (L) of 10 mm, and the width of the kernel (H) of 5 mm, the structure of which is shown in Figure 2c.

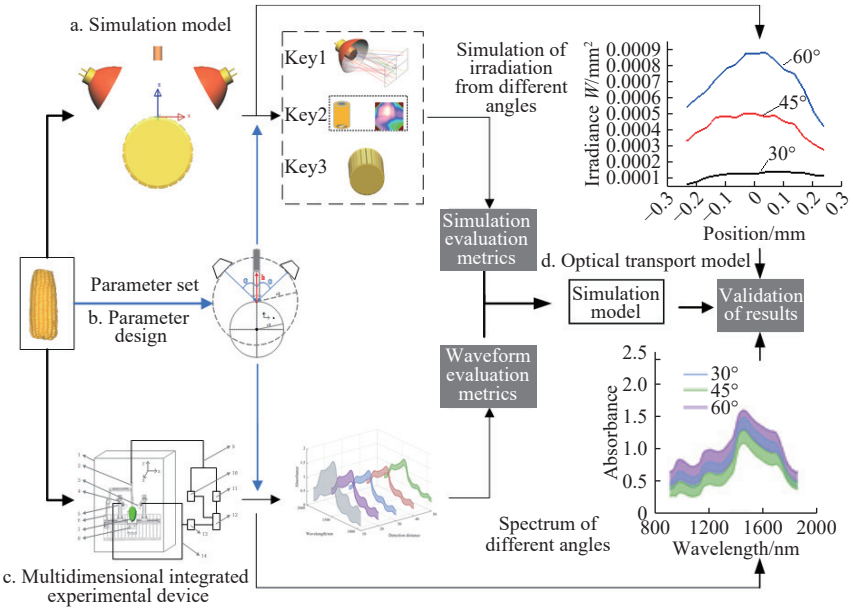

Figure 1 Framework diagram of the simulation process

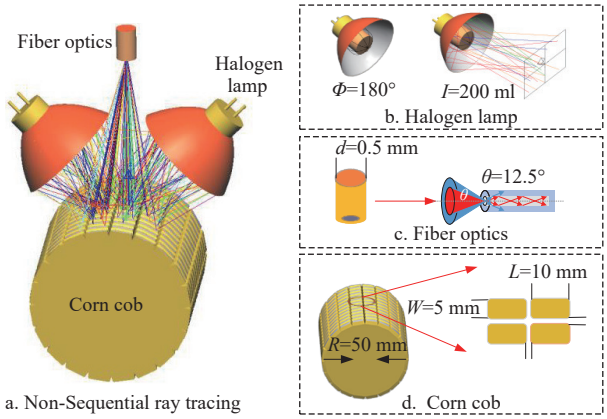

Figure 2 Settings of simulation parameters

The origin of the coordinate axis was set at the center of the maize cob, and the centerline of the fiber optic detector was perpendicular to the *Z*-axis. By adjusting the *Z*-axis coordinates, detection at different distances *h* can be realized. The halogen lamp light source is in the same plane as the fiber optic probe, and the angle between the halogen lamp and the fiber optic probe is used to define different angles of the incident light source. The angle of the incident light source is changed by adjusting the clamp angle as shown in Figure 1b. The experiment was conducted by diffuse reflection detection using a homemade multidimensional integrated experimental setup as shown in Figure 1c. Fresh maize spectral data were collected at different distances (10 mm, 20 mm, 30 mm, 40 mm, 50 mm) and different light source angles (30°, 45°, 60°), and the spectral area polarization was calculated. In order to match the appropriate optical properties of fresh maize cobs, the experimental and simulation data were verified and fitted as shown in Figure 1d. Finally, the optical properties of fresh maize were estimated by minimizing the relative errors of irradiation uniformity and spectral area polarization.

2.2 Attribute measurement

Optical characterization parameters of fresh maize include absorption and scattering coefficients and anisotropy factor (*g*). *g* is a dimensionless parameter characterizing the inhomogeneity of the light distribution in the tissue and the probability of forward scattering, taking values in the range [–1,1]. Most of the fruit and vegetable food and produce tissues *g* range in 0.7-0.9. This paper selected the reference value of 0.85 to approximate moisture content and cellular structure of fruit and vegetable tissues (such as apples, citrus) in the 900-1700 nm band of optical properties. The related research anisotropy factor *g* is between 0.8-0.9[31,32], so this paper takes a compromise value of 0.85. Since light is anisotropic during propagation, a reduced scattering coefficient (μ_s') is used[33,34]. Light reflects, scatters, absorbs, and transmits on the surface of the sample[35], which are shown in Figure 3. The backward scattering of the seeds is the diffuse signal received by the detector.

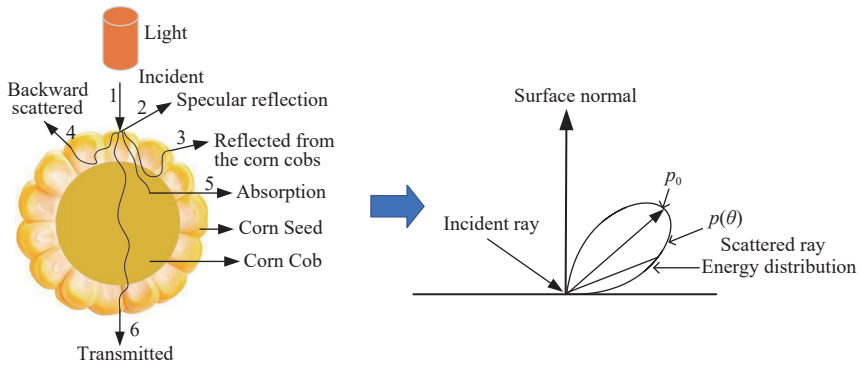

Note: 1 Incident light, 2 Specular reflection, 3 Reflected light from the maize cobs, 4 Backward scattered, 5 Absorption, 6 Transmitted

Figure 3 MCML simulation of light interaction with fresh maize tissues

Absorption of light by fresh maize cobs is mainly due to the functional groups of the chemical constituents. Scattering is mainly due to inhomogeneous refractive indices of the tissue components. The absorption coefficient μ_a represents the optical energy lost per unit path of photon due to absorption. The scattering coefficient μ_s expresses the optical energy d_z lost by photons on path dh_s due to scattering[36]. The formulas are given in (1)(2)(3) and common units are mm^{-1} or cm^{-1}.

$$\mu_a = \frac{dh_a}{d_z} \tag{1}$$

$$\mu_s = \frac{dh_s}{d_z} \tag{2}$$

$$\mu_s' = \mu_s(1-g) \tag{3}$$

Monte Carlo methods are used to capture the average behavior of light traces and describe the optical properties (reflectance, transmittance) of the sample. During the simulation, individual photons are gradually tracked through the sample medium while the light distribution characteristics are recorded. The parameters of each step (e.g., step size, scattering direction, photon energy, internal reflection, and boundary effects) are computed from known or estimated distributions by means of a random number function. The optical properties of the kernels of the fresh maize cob were set to elliptical Gaussian scattering, while the cob portion was set to full absorption and no scattering. Elliptical Gaussian scatterers are similar to conventional Gaussian scatterers. The difference, however, is that the former can model anisotropic distributions (i.e., non-rotational symmetry). The energy scattering distribution of an elliptical Gaussian scatterer can be described by the following Equation (4)[37]:

$$p(\theta) = p_0 exp\left[\left(-\frac{\theta}{2}\right)\left(\frac{\cos^2\phi}{\sigma_x^2}+\frac{\sin^2\phi}{\sigma_y^2}\right)\right] \tag{4}$$

θ is the scattering angle, also the angle of deviation from the direction of incidence; the larger θ, the faster the scattering intensity decays. $p(\theta)$ is the intensity in the theta direction and p_0 is the maximum intensity of the scattered intensity in the specular direction; σ_x, σ_y denote the standard deviation of the Gaussian distribution in the direction of the elliptical principal axes (long and short axes), respectively, controlling for anisotropy. If $\sigma_x \neq \sigma_y$ then it exhibits anisotropic scattering. ϕ is the azimuthal scattering angle in the cosine space direction; $\left(\frac{\cos^2\phi}{\sigma_x^2}+\frac{\sin^2\phi}{\sigma_y^2}\right)$ determines the directional dependence of the scattered intensity. When ϕ=0, the intensity is dominated by σ_x; when ϕ = 90°, the intensity is dominated by σ_y.

The elliptic Gaussian model allows defining the ratio between the absorption and scattering coefficients of the scatterer, thus regulating the diffuse reflection and transmission components of the energy partitioning relation of the light propagation process in the sample. Absorption (A) denotes the percentage of energy absorbed by the scatterer, while propagation (C) refers to the percentage of energy transmitted or reflected by the scatterer, and both satisfy A+C=100%. Reflection (R) refers to the percentage of energy reflected by the scatterer, and transmission (T) refers to the percentage of transmitted energy that passes through the surface, both of which satisfy R+T=100%. Diffuse reflection (D) represents the percentage of propagating reflected energy calculated according to the Lambertian scatterer model, where light is scattered around a surface normal around the point of incidence. The Gaussian component (G) refers to the propagated reflected energy, obeys a Gaussian distribution, has a standard deviation in degrees, and D+G=100%. When a photon enters the tissue, each time the photon moves one random step, partial absorption and scattering occurs due to collisions with the maize tissue particles, resulting in a gradual decrease in the weight of the photon. The weights w of the photons are updated according to Equation (5)[19]:

$$w' = w \times \frac{\mu_s}{\mu_s + \mu_a} \tag{5}$$

where, μ_a is the coefficient factor of the tissue; μ_s is the scattering coefficient of the tissue.

2.3 Simulation experimental design

According to the diffuse reflectance spectra of fresh maize cobs obtained from the near-infrared detection system, the variation range of absorptivity was statistically analyzed to be 0.2-1.2, and the step size of absorptivity was 0.2. The transmittance is then calculated according to the formula. Transmittance T of 63%, 25%, and 6%, respectively, corresponds to the propagation rate in the elliptic Gaussian model. First, the propagation rate is set to 63%, 25%, and 6%, respectively, and the corresponding absorption rates are calculated by the simulation software to be 37%, 75%, and 5%, respectively. The variation range of reflectance is set to 20%-100% (in steps of 20%). At this point, the diffuse reflectance D is 100% and the Gaussian component G is 0%. By calculating the detection irradiance uniformity at different detection distances for different reflectivities R and transmittances T, three sets of data were obtained, totaling 60 data points. Then, the irradiation uniformity was based on the minimum relative error of the polar aberration of the spectral area for each optical parameter. The optimal A, R, and T values were matched. On this basis, the variation range of diffuse reflectance was set to 20%-100% (in steps of 20%). Calculate the detection irradiance uniformity for different detection distances at different D values. Get one set of data with 20 data points and match the D-value in the same way.

2.4 Physical test verification

2.4.1 Disposable material

Wan Nuo 2000 fresh maize was used, which was picked in the morning of the right season in the field of Wuqing, Tianjin, and transported to the laboratory in time to be stored in the refrigerator. The bracts were manually peeled off, maize whiskers and cob shanks were removed, and 80 cobs of uniform size, full kernels, and free of pests and diseases were selected as samples.

2.4.2 Test equipment

Near-infrared spectral acquisition of fresh maize cobs was performed using a homemade synthesized device, defining the middle surface of the cob as the sampling area and marking it with a marker pen, as shown in Figure 4a. The middle of the cob is below the fiber optic probe. Adjust the mechanical device so that the central axis of the cob is parallel to the Z-axis, the central axis of the fiber optic probe is parallel to the Y-axis, the material around the halogen lamp to the fiber optic probe is as the axis of symmetry of the row, and the three are in the same plane and perpendicular to the Z-axis, as shown in Figure 4b. The distance between the fiber optic probe and the material is defined as h, the angle with the fiber optic probe is defined as θ, and the halogen lamp light source has 20 W power.

2.4.3 Data acquisition

Defining the middle surface of the cob as the sampling area, a circular rotation was made along the cob's central axis, with the angle of rotation randomized each time, and 360° for each type of

trial. The spectra were collected at probe distances h of 10 mm, 20 mm, 30 mm, 40 mm, and 50 mm and at light source angles θ of 30°, 45°, and 60°, respectively. The average spectrum obtained by averaging the respective spectra was then obtained. Modeling validation tests for each type of different configuration parameters for each sample measured three times, three times the average of the spectra as the original spectra of the sample, then 80 samples 30° and 45° test were measured 240 times, for a total of 480 data points.

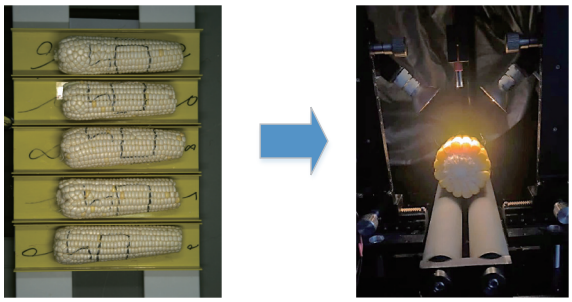

a. Fruit cob samples b. Spectral acquisition

Figure 4 Acquisition device

2.4.4 Data processing

Firstly, the sample set partitioning based on joint x-y distance (SPXY) was used to partition the fresh maize samples. The spectral preprocessing of the fresh maize sample spectra was then performed using the Standard Normal Variate (SNV) transformation. Finally, Support Vector Machines (SVM) algorithm was used to correlate the spectral information with the physical and chemical values of water content to establish a quantitative analysis and detection model for water content of fresh maize. SVM has strong generalization ability, but it is susceptible to kernel function. Common kernel functions include linear kernel, RBF kernel, Gaussian kernel, and polynomial kernel. In this paper, linear kernel is used to construct SVM, and its kernel function is $k(x,x')=x^T\times x'$, and the core parameter is the penalty parameter C. The larger the value of C, the lower the model's tolerance to misclassification, which may lead to overfitting; the smaller the value of C, the higher the model's tolerance to misclassification, which may lead to underfitting. In order to obtain the optimal C value, the particle swarm optimization algorithm (PSO) is used to automatically find the appropriate penalty parameter C. The parameters in this paper are set as follows: the number of particles N=30, the maximum number of iterations T_{max} =30, the minimum value of the penalty parameter C_{min} =0.1, and the maximum value of the penalty parameter C_{max} = 100, and the final optimized C value is 10.5.

2.5 Evaluation indicator design

2.5.1 Simulation evaluation metrics

Irradiance surface uniformity[38] is the relative standard deviation of irradiance at different locations of the outlet plane calculated as in Equation (6):

$$U=1-\mathrm{std}(E_i)/\bar{E}\times 100\% \tag{6}$$

where, U is the irradiance uniformity; E_i is the value of irradiance without using location; $\bar{E}$ is the mean value of irradiance at different locations; $\mathrm{std}(E_i)$ is the standard deviation of irradiance at different locations.

2.5.2 Waveform evaluation metrics

The spectral area extreme deviation is defined as the cumulative sum of the curve areas between the highest and lowest values of absorbance corresponding to each spectral point of a set of spectral curves[39], which is calculated as shown in Equation (7).

$$SAD=\sum_{i=1}^{N-1}\frac{\left(X_{\max,i}-X_{\min,i}\right)+\left(X_{\max,i+1}-X_{\min,i+1}\right)}{2}\times\Delta\lambda_i \tag{7}$$

where, SAD is the differential integral absorbance; X_i is the spectral value at each wavelength point; $\bar{X}$ is the overall average spectral value; N is the total number of wavelength points; $X_{\max,i}$ is the absorbance of the highest spectra at the first wavelength point; $X_{\min,i}$ is the absorbance of the lowest spectra at the first wavelength point; and $\Delta\lambda_i$ is the distance between neighboring wavelengths.

The performance of the constructed model was evaluated by correlation coefficient R^2, Root Mean Square Error (RMSE), and Residual Predictive Deviation (RPD)[33], which were calculated as shown in Equations (8)-(10):

$$R^2=1-\frac{\sum(y_i-\hat{y}_i)^2}{\sum(y_i-\bar{y})^2} \tag{8}$$

$$\mathrm{RMSE}=\sqrt{\frac{\sum_{i=1}^{n}(y_i-\hat{y}_i)^2}{n-1}} \tag{9}$$

$$\mathrm{RPD}=\frac{\mathrm{SD}}{\mathrm{RMSEP}} \tag{10}$$

where, SD is the standard deviation of the sample content of the prediction set.

3 Results and discussion

3.1 Maize optical properties simulation results

3.1.1 Comparative analysis of different A, R, and T rates

Figure 5a shows the average spectra at 45° incidence angle for different detection distances, and the average spectra at different distances are statistically analyzed. Spectral area extremes were counted and were 697.8, 312.5, 199.0, 87.2, and 145.7, respectively. The differences between the different distances were 385.3, 113.5, 11.8, and 41.5, in that order. The relative rates of change were 123.3%, 57.0%, 6.3%, and 28.5%, respectively. The results show that the spectral amplitude decreases with increasing detection distance in the range of 10 mm to 40 mm, while the amplitude at 50 mm lies between 20 mm and 30 mm. Figure 5b, 5c, and 5d demonstrate U for different detection distances at 45° with different optical parameter settings (absorptivity A, propagation C, reflectivity R, transmittance T). The results show that the trend of U change is more or less the same. However, the amplitude difference is large. At 10 mm and 20 mm, the detection distance is too close, with a large scattering of light, higher U but relatively low luminous flux. The received optical power was 0.002 85 W and 0.0068 W, respectively. Therefore the main match is a regular trend between 30 mm and 50 mm. It can be seen that as the reflectivity R increases, U also increases. However, there is significant variability in the degree of U attenuation at different detection distances as the absorptivity A increases.

In order to accurately match the optical property parameters (absorptivity A, reflectance R, transmittance T) of fresh maize cobs, a conclusion can be drawn by analyzing the relative error between the relative rate of change of spectral area polarization (SADR) and the relative rate of change of irradiance uniformity (UR) for different optical properties. As shown in Figure 6, the optical attribute parameters corresponding to the smallest relative error, those that best fit the characteristics of the fresh maize cob, are shown to be A=37%, T=20%, and R=80%.

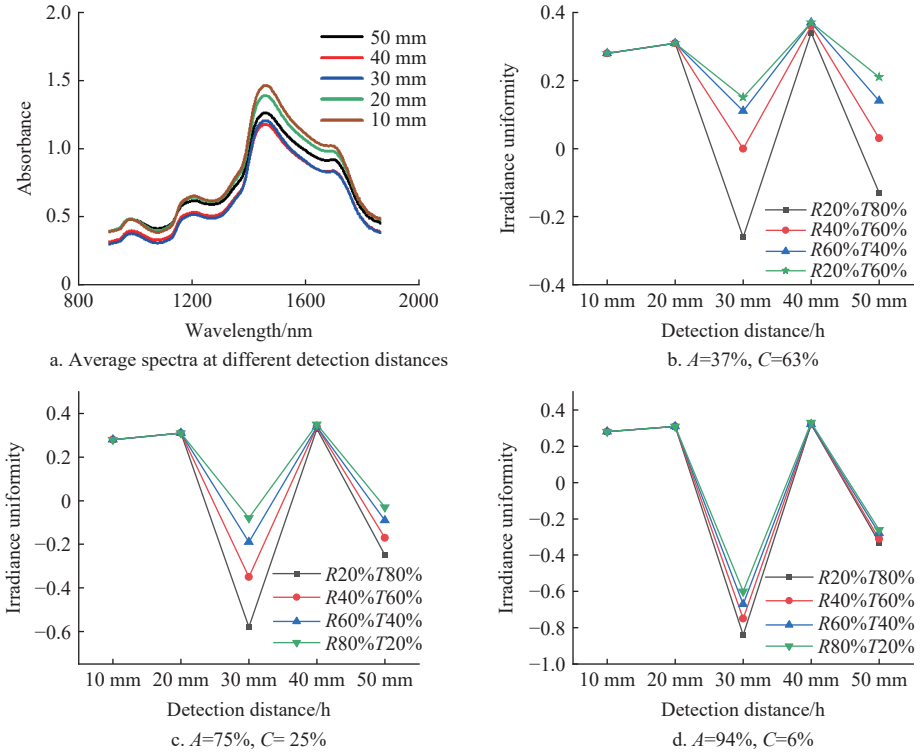

a. Average spectra at different detection distances

b. A=37%, C=63%

c. A=75%, C= 25%

d. A=94%, C=6%

Figure 5 Irradiation uniformity at different absorptivity rates

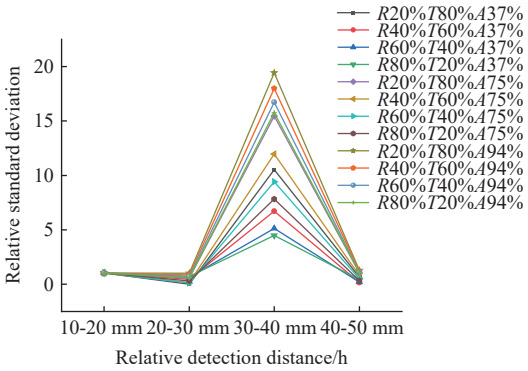

Figure 6 Relative detection distance error for different absorption rates

3.1.2 Comparative analysis of different diffuse reflectance rates

The optical properties of fresh maize cobs were identified in Section 3.1.1 as: absorptivity A=37%, transmittance T=20%, and reflectance R=80%, where R=80% contains forward scattering (G) and diffuse reflection (D). Thus, the contribution of diffuse reflections is further distinguished. As shown in Figure 7, there is a large difference in U between different detection distances for different D values. Calculating the average error of the relative error under different reflectance combinations gives the following results: when D=20% and G=80%, the average error is 108%; when D=40% and G=60%, the average error is 52.94%; when D=60% and G=40, the average error is 63.77%; and when D=20% and G=80%, the average error is 53.19%. From the results, it can be seen that the average error is the smallest when D=40% and G=60%, so this parameter is the most matching parameter for this model, as shown in Figure 8. The spectral information measured by NIR spectroscopy is a combination of light absorption and scattering. However the exact mechanism of interaction between light and tissue is not clear[11]. For this reason, this paper analyzes the interaction between fresh maize cob and light by means of optical simulation of the inversion. The results show that the proportion of reflected light accounted for by the diffuse reflection of the kernel was analyzed, A=37%, T=20%, and D=40%.

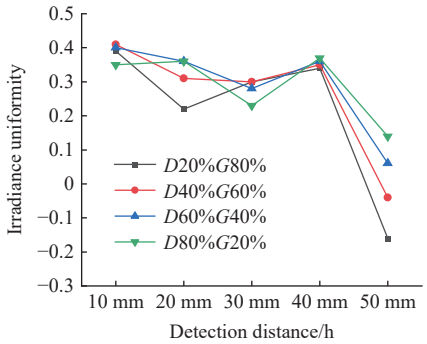

Figure 7 Diffuse reflection parameter difference

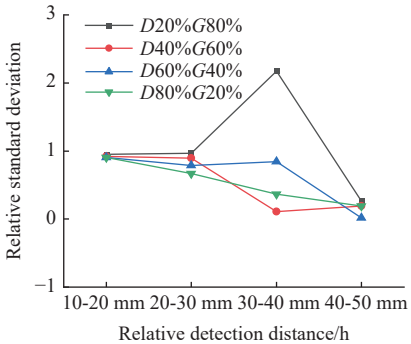

Figure 8 Relative differences of diffuse reflection parameters

3.2 Verification of optical properties of maize cob

From Section 3.1, the optical properties of fresh maize cob are: absorptivity A=37%, transmittance T=20%, reflectance R=80%, diffuse reflectance D=40%, and Gaussian reflectance G=60%. In acquiring NIR spectra, the middle surface of the cob was defined as the sampling area and rotated circumferentially along the cob's central axis. The angle of each rotation was randomized, so the

optical simulation model for fresh maize was rotated accordingly in the LightTools software. Specifically, the simulation is set up for the following five scenarios: the center is located in the center of the seed; the center is located between the transverse axial gaps of the seed; the center is located halfway between the transverse axial gaps of the seed and the surface of the seed; the center is located between the longitudinal axial gaps of the seed; the center is located halfway between the longitudinal axial gaps of the seed and the surface of the seed. Simulate U at different distances under dynamics and find the relative change in its value. Under the cob dynamics, the relative trends of the mean values of U and SADR were consistent, as shown in Figure 9, which verified the accuracy of the optical attributes of fresh maize cobs.

Figure10a shows the average spectra collected when the light source angle θ is 30°, 45°, 60°, and the detection distance h is 40 mm. The trends of the overall curves were consistent, but there was significant variance in the magnitude of absorbance. Statistical analysis of spectra is required from different angles. The results show that the spectral area polar deviation and standard deviation gradually become larger as the angle of clamping increases. The standard deviation was less than 1 for both 30° and 45°, and 1.24 for 60°. The simulation results are that 45° has the highest U, followed by 30°, and the worst is 60°, as listed in Table 1. The simulation results are consistent with the change rule of spectral statistics, which further verifies the rationality of the optical properties.

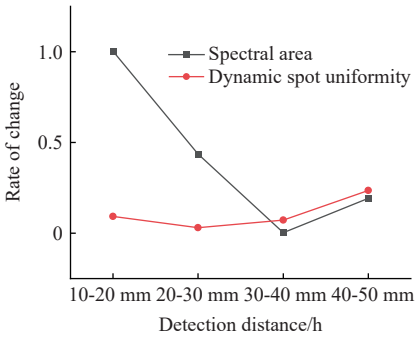

Figure 9 Relative changes in irradiation uniformity

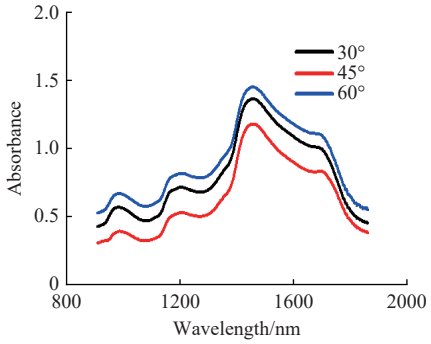

a. Spectrum averaged over different angles

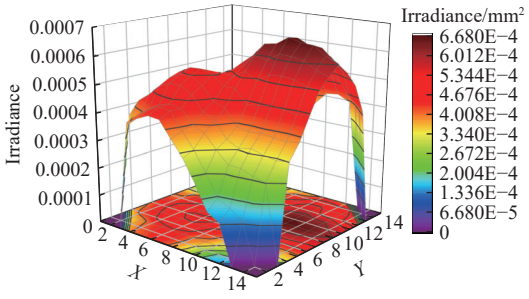

b. Spot diagram of 60° irradiation

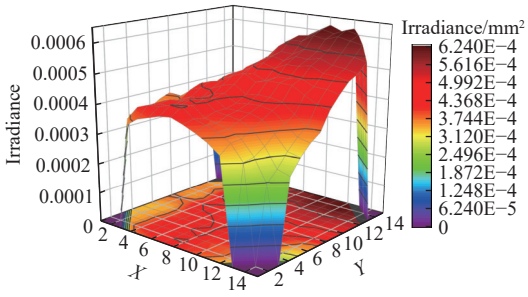

c. Spot diagram of 45° irradiation

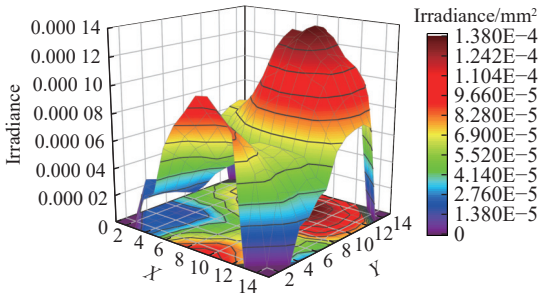

d. Spot diagram of 30° irradiation

Figure 10 Irradiated light spot map at different angles

Table 1 Statistical analysis of different light source angles and irradiance uniformity

Angle	Spectral area extreme difference	Standard deviation	Irradiance uniformity
30°	149.2	0.57	50%
45°	187.2	0.83	54%
60°	291.4	1.24	42%

The optical properties of fresh maize cobs were evaluated by simulation as A=37%, T=20%, D=40%. When the light intensity enters the interior of the maize cob, 37% of the light intensity is absorbed by the chemical composition of the cob, 20% is transmitted through the maize kernel, and 40% is accepted by the detector on a diffusely reflecting surface. Figure 9 shows the irradiated spot map received by the detector at a detection distance of 40 mm and light source angles of 60°, 45°, and 30°.

3.3 Simulation results analysis

As shown in Figure 11a, there is a significant difference in the detector received luminous flux at different detection distances. The highest luminous flux was found at 10 mm and 40 mm, followed by 20 mm and 50 mm, and the lowest received flux was found at 30 mm, which indicates that the signal strength is weakest at this distance condition. The spike response area varied with increasing detection distance. Figure 11b-11f show the received irradiated spot maps for 10 mm, 20 mm, 30 mm, 40 mm, and 50 mm detectors, respectively. It was found that at a detection distance of 40 mm and a light source angle of 45°, the luminous flux was higher and centered, and the top of the seed could cover more light, so the detector not only obtained more information but was also more

comprehensive. Therefore, the detection distance of 40 mm and the light source angle of 45° can obtain the information of the top of the grain more stably and thus have a certain superiority in modeling effect.

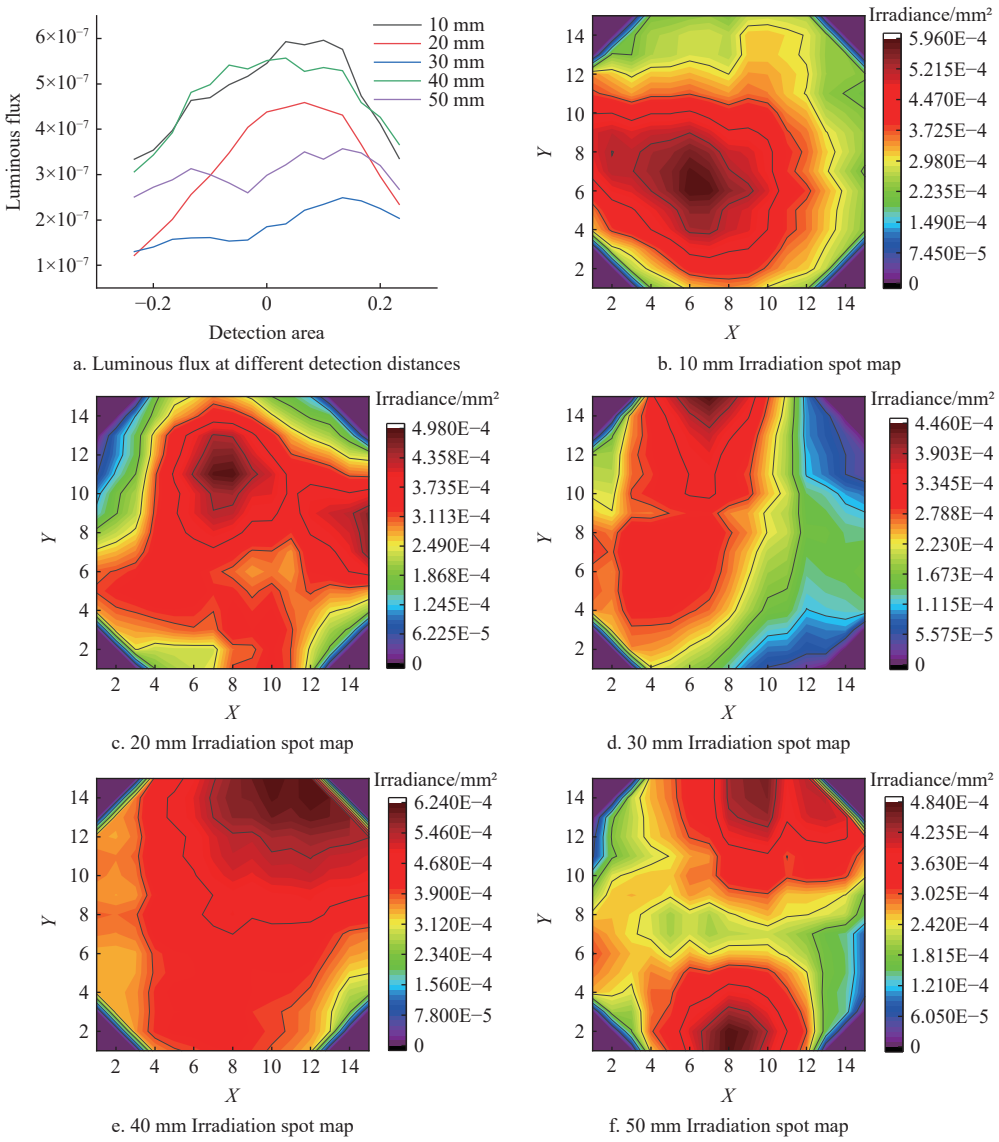

a. Luminous flux at different detection distances

b. 10 mm Irradiation spot map

c. 20 mm Irradiation spot map

d. 30 mm Irradiation spot map

e. 40 mm Irradiation spot map

f. 50 mm Irradiation spot map

Figure 11 Irradiated spot and luminous flux at different detection distances

3.4 Analysis of modeling results

The water content of fresh maize cobs was modeled with a detection distance of 40 mm and light source angles of 30° and 45°, and the effects of different optical structures on the water content detection accuracy of fresh maize cobs were analyzed. The SNV-SVM model was used to predict the water content of fresh maize cobs, and the results are listed in Table 2. Comparing the modeling accuracies at 30° and 45°, the R_P^2 and RPD values of the modeling results at 45° were 0.880 and 2.956, respectively, and those at 30° were 0.845 and 2.608, respectively. R_P^2 is 4% higher than the 30° angle, and the RPD is 0.348 higher than the 30° angle; therefore, 45° modeling is better than 30°. According to the standards related to the spectral detection of grains, the coefficient of determination is required to be greater than 0.85 to meet the accuracy requirements of daily detection, and the model prediction performance is better when the RPD is >2.5, which can be used for preliminary prediction applications in practice[40]. It can be used for quantitative analysis and has the potential for practical application, but the accuracy needs to be further improved to provide a technical basis for the development of near-infrared detection of fresh maize.

Table 2 Results of water content modeling test of fresh maize at different angles

Angle	Model	Pre-processing	Calibration set		Prediction set		
			R_C^2	RMSEC	R_P^2	RMSEC	RPD
30°	SVM	SNV	0.945	0.697	0.845	0.910	2.608
45°	SVM	SNV	0.943	0.708	0.880	0.932	2.956

4 Conclusions

This study evaluated the optical properties of fresh maize cobs based on their diffuse reflectance spectral signals under different collection conditions and explored the effect of multiple optical structures on the prediction model of fresh maize water content. A support vector machine (SVM) combined with a spectral preprocessing technique (SNV) was used for modeling. The conclusions are as follows:

Development of an optical simulation model for fresh maize cobs. The uniformity of irradiation received by the detector under different optical configurations was optically simulated to match the degree of attenuation of the diffusely reflected signals from the

actual collected cob. The optical properties of fresh maize cobs were matched to *A*=37%, *T*=20%, and *D*=40%.

Modeling the water content of fresh maize cobs at a detection distance of 40 mm and light source angles of 30° and 45° using SNV+SVM. 45° modeling is better than 30°. Optical simulations verified that more stable access to the top of the seed could be obtained at a detection distance of 40 mm and a light source angle of 45°.

This study provides a reference for understanding the relationship between the optical properties of fresh maize cobs and the detection of optical structures by contributing to the understanding of light interactions with fresh maize cobs and analyzing the mechanism of model prediction of water content. It also contributes to the development of more effective NDT methods. In the future, the actual optical measurement methods can be combined to systematically analyze the influence of curvature change, arrangement and epidermal structure of the maize kernel surface on the light propagation path, scattering intensity distribution and diffuse reflection signal acquisition stability in different wavelength bands, so as to improve the applicability of the water content prediction model and the accuracy of the detection.

Acknowledgements

This work was supported by the National Key Research and Development Program of China (Grant No. 2023YFD2001301); the Independent Research and Development Project of Academy of Agricultural Planning and Engineering, Ministry of Agriculture and Rural Affairs (Grant No. SP202402); and the Key Laboratory of Agro-Products Primary Processing, Ministry of Agriculture and Rural Affairs (Grant No. KLAPPP2024-01).

[References]

[1] An L, Cheng Y, Luo S K, Zhou G Q, Han X A, Song B. Research progress on nutritional quality of fresh waxy corn and its influencing factors. Journal of Mountain Agriculture and Biology, 2023; 42(5): 40–45. (in Chinese)

[2] Xu L, Zhao J R, Lu B S, Shi Y X, Fan Y L. Current situation and development trend of fresh corn seed industry in China. China Seed Industry, 2020(10): 14–18. (in Chinese)

[3] Yang X H, Zhu L C, Huang X, Zhang Q, Li S, Chen Q L, et al. Determination of the soluble solids content in korla fragrant pears based on visible and near-infrared spectroscopy combined with model analysis and variable selection. Frontiers in Plant Science, 2022; 13: 938162.

[4] Peng D, Liu Y L, Yang J S, Bi Y L, Chen J N. Nondestructive detection of moisture content in walnut kernel by near‐infrared diffuse reflectance spectroscopy. Journal of Spectroscopy, 2021; 2021(1): 9986940.

[5] Yang Q N, Yang X H, Zhang Q L, Wang Y B, Song H, Huang F R. Quantifying soluble sugar in super sweet corn using near-infrared spectroscopy combined with chemometrics. Optik, 2020; 220: 165128.

[6] Semyalo D, Kwon O, Wakholi C, Min H J, Cho B K. Nondestructive online measurement of pineapple maturity and soluble solids content using visible and near-infrared spectral analysis. Postharvest Biology and Technology, 2024; 209: 112706.

[7] An M, Cao C, Wang S, Zhang X C, Ding W Y. Non-destructive identification of moldy walnut based on NIR. Journal of Food Composition & Analysis, 2023; 121: 105407.

[8] Li X, Zhong Y, Li J, Lin Z Z, Pei Y L, Dai S Y, et al. Rapid identification and determination of adulteration in medicinal Arnebiae Radix by combining near infrared spectroscopy with chemometrics. Spectrochimica Acta Part A: Molecular and Biomolecular Spectroscopy, 2024; 318: 124437.

[9] Hu D, Fu X P, Wang A C, Ying Y B. Measurement methods for optical absorption and scattering properties of fruits and vegetables. Transactions of the ASABE, 2015; 58(5): 1387–1401.

[10] Wang Z, Hu D, Sun Z Z, Ying Y Y. Application status and perspective of spatial-frequency domain imaging in quality evaluation of agricultural products. Agricultural Engineering, 2021; 37(15): 275–288.

[11] Sun Z Z, Hu D, Zhou T T, Sun X L, Xie L J, Ying Y B. Development of a multispectral spatial-frequency domain imaging system for property and quality assessment of fruits and vegetables. Computers and Electronics in Agriculture, 2023; 214: 108251.

[12] Tian S J, Xu H R. Nondestructive methods for the quality assessmen.t of fruits and vegetables considering their physical and biological variability. Food Engineering Reviews, 2022; 14(3): 380–407.

[13] Yang S H, Tian Q J, Wang Z W, Guo W C. Relationship between optical properties and internal quality of melon tissues during storage and simulation-based optimization of spectral detection in diffuse reflectance mode. Postharvest Biology and Technology, 2024; 213: 112935.

[14] Tang C X, Wang Z R, Li E B. Study on the distribution characteristics of scattered light around peach pit. Journal of Agricultural Science and Technology, 2016; 18(4): 79–86. (in Chinese)

[15] Teet S E, Hashim N. Recent advances of application of optical imaging techniques for disease detection in fruits and vegetables: A review. Food Control, 2023; 152: 109849.

[16] Pan L Q, Fang L, Zhou B J, Zhang B, Ping J, Tu K. System and principle of optical properties measurement and advances on quality detection of fruits and vegetables. Journal of Nanjing Agricultural University, 2021; 44(3): 401–411.

[17] Lv C Y, Zhan R J. Measurement method of optical property parameters of biological tissue. Laser & Optoelectronics Progress, 2021; 58(3): 0300004–30000458.

[18] Shi Z, Anderson C A. Application of Monte Carlo simulation-based photon migration for enhanced understanding of near-infrared (NIR) diffuse reflectance. Part I: Depth of penetration in pharmaceutical materials. Journal of Pharmaceutical Sciences, 2010; 99(5): 2399–2412.

[19] Zhou Y H, Guo W C, Ji T K, Du R Y. Low-cost and handheld detector on soluble solids content and firmness of kiwifruit. Infrared Physics & Technology, 2023; 131: 104641.

[20] Zhang S X, Xu H L, Wang J B, Sun Y X, Wang H Y. Detection of watercore disease in apple based on inversion of optical characteristic parameters. Journal of Nanjing Agricultural University, 2023; 46(5): 986–994. (in Chinese)

[21] Tan Z J, Ding C Z. Semi-empirical model for diffuse reflectance from homogeneous spherical turbid media measured via small diameter detectors. Journal of Modern Optics, 2017; 64(18): 1885–1891.

[22] Light tools software introduction. Available: https://www.synopsys.com/. Accessed on [2025-06-25]

[23] Vaudelle F, L'Huillier J P. Influence of the size and skin thickness of apple varieties on the retrieval of internal optical properties using Vis/NIR spectroscopy: A Monte Carlo-based study. Computers and Electronics in Agriculture, 2015; 116: 137–149.

[24] He X M, Fu X, Li T W, Rao X Q. Spatial frequency domain imaging for detecting bruises of pears. Journal of Food Measurement and Characterization, 2018; 12: 1266–1273.

[25] Özcan M K, Gökçe M C, Baykal Y. Transmittance of Gaussian beams in biological tissues. Journal of Quantitative Spectroscopy and Radiative Transfer, 2025; 333: 109312.

[26] Yang M, Sun Q C, Hou H Y. Design of fiber optics probe based on monte carlo simulation and application of the probe in fluorescence spectrum measurement of nicotinamide adenine dinucleotide in Skin. Laser & Optoelectronics Progress, 2021; 58(22): 433–440. (in Chinese)

[27] Qiao W Y, Gao Z S, Yuan Q, Zhu D, Xu N Y, Lun X L, et al. Scattered ray tracing based on rejection sampling method with BRDF discrete numerical value. Acta Photonica Sinica, 2023; 52(4): 0429001.

[28] Misran M A B, Bilgaiyan A, Hattori R. Optical ray tracing simulation by using monte carlo method for reflectance-based photoplethysmography sensor in human skin and fingertip model. Computational And Experimental Research In Materials And Renewable Energy, 2022; 5(2): 78–91.

[29] Sun J, Künnemeyer R, McGlone A, Tomer N. Investigations of optical geometry and sample positioning in NIRS transmittance for detecting vascular browning in apples. Computers and Electronics in Agriculture, 2018; 155: 32–40.

[30] Han C, Yin J F, Hao T, Yan J S, Xu H R. Evaluation of the optical layout and sample size on online detection of apple watercore and SSC using Vis/NIR spectroscopy. Food Composition and Analysis, 2023; 123: 105528.

[31] Sun C, Beers R V, Aernouts B, Saeys W. Bulk optical properties of citrus tissues and the relationship with quality properties. Postharvest Biology

and Technology, 2020; 163: 111127.

[32] Xie D D, Liu D Y, Guo W C. Relationship of the optical properties with soluble solids content and moisture content of strawberry during ripening. Postharvest Biology and Technology, 2021; 179: 111569.

[33] Qin J W, Lu R F. Measurement of the optical properties of fruits and vegetables using spatially resolved hyperspectral diffuse reflectance imaging technique. Postharvest Biology and Technology, 2008; 49(3): 355–365.

[34] Sun X L, Zhou T T, Sun Z Z, Li Z M, Hu D. Research progress into optical property-based nondestructive fruit and vegetable quality assessment. Food Research & Development, 2022; 43(4): 209–218. (in Chinese)

[35] Gao Y W, Geng J F, Rao X Q. Non-invasive bruise detection in postharvest fruits and vegetables: A review. 2017; 38(15): 277–287. (in Chinese) doi: 10.7506/spkx1002-6630-201715044.

[36] Xu G, Dong L Q, Kong L G, Zhao Y J, Liu M, Hui M, et al. Parameters inversion algorithm of biological tissues based on a neural network model. Acta Optica Sinica, 2021; 41(11): 1117001. (in Chinese)

[37] Chong W, Lyu W H, Zhang J, Liang J, Yang X T, Liu S, et al. Calibration system of sunshine duration recorder based on Bi-Xenon lamp source integrating sphere. Acta Optica Sinica, 2022; 42(1): 0112004. (in Chinese)

[38] Zhang Y L, Yang G H, Wang M P, Han Z Y, Zhu G F, Shi J F, et al. Factors affecting the non-destructive detection of water contents in fresh corn cobs by near-infrared spectroscopy. Transactions of the CSAE, 2024; 40(15): 262–270. (in Chinese)

[39] Liu W H, Han Y N, Wang N, Zhang Z, Wang Q G, Miao Y P. Apple sugar content non-destructive detection device based on near-infrared multi-characteristic wavelength. Journal of Physics: Conference Series. IOP Publishing, 2022; 2221: 012012.

[40] Shen F, Liu X, Pei F, Li P, Jiang D F, Liu Q. Rapid identification of deoxynivalenol contamination in wheat and its products by attenuated total reflectance-Fourier transform infrared spectroscopy (ATR-FTIR). Food Science, 2019; 40(2): 293–297. (in Chinese)